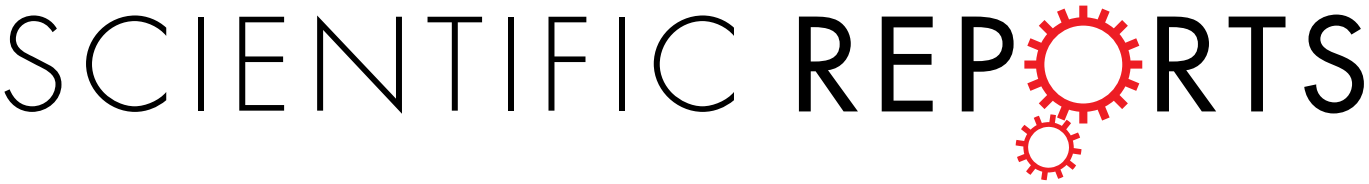

OPEN

Phonon Boost Effect on the $S^{\pm}$-wave Superconductor with Incipient Band

Received: 12 September 2018
Accepted: 19 February 2019
Published online: 07 March 2019

Yunkyu Bang[1,2]

We showed that the all phonons – not only forward-scattering phonon but also local (all-momentum-scattering) phonon – contribute to boosting *Tc* of the $S^{\pm}$-wave pairing state in the incipient band model. In particular, when the incipient band sinks deeper, the phonon boost effect of the local phonon increases and becomes as effective as the one of the forward-scattering phonon. Our finding implies that all interface phonons from the $SrTiO_3$ substrate – not only the 90 *meV* Fuchs-Kliewer (F-K) phonon but also the 60 *meV* F-K phonon – as well as all intrinsic phonons of the FeSe monolayer itself, regardless of their degree of "*forwardness*", should contribute to increase *Tc* of the FeSe/STO monolayer system. This all-phonon boost mechanism should universally work in all heavily doped (either by holes or by electrons) Iron-based superconductors.

The discovery of the FeSe/$SrTiO_3$ monolayer system ($T_c \approx 60$–$100\,K$)[1–3] is posing a serious challenge to our understanding of the Iron-based superconductors (IBS)[4–6]. As to the origin of such a high T_c value, it is widely accepted that the forward-scattering phonon, penetrating from the $SrTiO_3$ substrate, is the key booster for increasing T_c[7–11]. Indeed, Lee *et al.*[7] have measured the replica band shifted by about 90 *meV* downward from the original electron band, and it was claimed to be a smoking-gun evidence for the presence of the forward-scattering phonon coupled to the conduction band electrons in the FeSe monolayer. Subsequently, the high-resolution electron energy loss spectroscopy (HREELS) measurement[12] has directly measured the 90 *meV* and 60 *meV* Fuchs-Kliewer (F-K) interface phonon modes in the FeSe/$SrTiO_3$(STO) system[12] besides several lower energy bulk phonon modes of FeSe layer. However, this HREELS experiment itself has no information about whether the observed F-K modes (both 90 *meV* and 60 *meV* modes) are forward-scattering or all-momentum scattering phonons.

Then, recently, Sawatzky and coworkers[13] have pointed that the replica band observed in the Angle Resolved Photo-Emission Spectroscopy (ARPES) experiment[7] is not the evidence of a forward-scattering phonon coupled to the conduction electrons of the FeSe layer but a consequence of the kinematics of the escaping electrons in the ARPES measurement. The main point of this criticism is that it is true that there exists a F-K phonon mode of the energy ~90 *meV*[12], but there is no evidence that this phonon is a small-momentum exchange (forward-scattering) phonon which produces the replica band by coupling to the main conduction band electrons of the FeSe layer; it may couple but via all-momentum exchange and in this case no replica band can be formed.

In this paper, we studied the effect of the generic types of phonons on the superconducting (SC) instability of the $s^{\pm}$-gap symmetry in the incipient band model. The incipient band model[14,15] has been introduced to study the superconductivity of the so-called heavily electron-doped iron selenide (HEDIS) compounds. All HEDIS compounds have the missing hole pocket (Fermi surface) because the hole band sinks below Fermi level by about ~60–90 *meV* due to the heavy electron doping, hence also called as an incipient band. Despite missing hole pocket, these compounds have achieved surprisingly high T_c values: $A_xFe_{2-y}Se_2$ (A = K, Rb, Cs, Tl, etc.) ($T_c \approx 30$–$40\,K$)[16–18] and $(Li_{1-x}Fe_xOH)FeSe$ ($T_c \approx 40\,K$)[19], and the FeSe/$SrTiO_3$ monolayer system ($T_c \approx 60$–$100\,K$)[1–3]. Therefore, the origin of these high T_c values of the HEDIS compounds or the incipient band system is a challenging mystery to be understood, and in particular it is curious to know whether the incipient band plays any active role to enhance T_c.

As to these questions, our study in current paper has found that the all phonons–not only forward-scattering phonon but also local (all-momentum-scattering) phonon–contribute to boost T_c of the incipient band superconductor. In particular, we showed that as the incipient band sinks deeper, the phonon boost effect of both types of phonon becomes indistinguishably similar from one another. It means that the sunken hole band plays an active

[1]Asia Pacific Center for Theoretical Physics, Pohang, Gyeongbuk, 790-784, Korea. [2]Department of Physics, POSTECH, Pohang, Gyeongbuk, 790-784, Korea. Correspondence and requests for materials should be addressed to Y.B. (email: ykbang@apctp.org)

role to turn otherwise useless phonons (all-momentum scattering phonons) into useful pairing glues. Our finding implies that all phonons[12], both interface phonons from the STO substrate (the 90 *meV* and 60 *meV* F-K phonons) and intrinsic phonons of the FeSe monolayer itself should contribute to increase T_c of the FeSe/STO monolayer system. This all-phonon boost mechanism should work in all heavily doped (either by holes or by electrons) Iron-based superconductors.

Results

Phonon Boost Mechanism. The underlying reason for this surprising result is because the relative size of Δ^+-gap and Δ^--gap of the $s^{\pm}$-wave pairing state in the incipient band superconductor is generically not equal, and this disparity of gap size grows as the incipient band sinks deeper. To illustrate the consequence of this effect, let us recollect the general principle of a phonon contribution to the unconventional superconductor with a sign-changing order parameter (OP) $\Delta(k)$, in general. In the BCS pairing theory with pairing interactions of $V_{sf}(k, k')$ and $V_{ph}(k, k')$, the gap equation at T_c with a gap function $\Delta(k)$ has the following structure

$$\begin{aligned}\Delta(k) &= -\sum_{k'} V_{sf}(k, k')\Delta(k')\chi_{sf}(T) \\ &\quad -\sum_{k'} V_{ph}(k, k')\Delta(k')\chi_{ph}(T),\end{aligned} \tag{1}$$

where $V_{sf}(k, k')(>0)$ is a repulsive spin-fluctuation mediated interaction and $V_{ph}(k, k')(<0)$ is an attractive phonon interaction. $\chi_{sf(ph)}(T)$ are the pair susceptibilities defined as $\chi_{sf}(T) = N(0)\int_{-\Lambda_{sf}}^{\Lambda_{sf}} d\xi \frac{\tanh\left(\frac{\xi}{2T}\right)}{2\xi}$ and $\chi_{ph}(T) = N(0)\int_{-\omega_D}^{\omega_D} d\xi \frac{\tanh\left(\frac{\xi}{2T}\right)}{2\xi} = N(0)\phi(T, \omega_D)$, respectively, where $\phi(T, \omega_D)$ is the result of the integral $\int_{-\omega_D}^{\omega_D} d\xi \ldots$. Assuming that the gap symmetry is already determined by the primary pairing interaction $V_{sf}(k, k')$, the second term of Eq. (1) defines the additional contribution from the phonon interaction $V_{ph}(k, k')$ to the total pairing as

$$\sum_{k'} V_{ph}(k, k')\Delta(k')\chi_{ph}(T) = \phi(T, \omega_D)N(0) < V_{ph}(k, k')\Delta(k') >_{k'}, \tag{2}$$

where $<\cdots>_k$ means the Fermi surface (FS) average. For example, the contribution of the local Einstein phonon interaction $V_{ph}(k, k') = V_0$ to the d-wave gap, $\Delta_d(k) \sim (\cos k_x - \cos k_y)$, would be null because

$$V_0 < \Delta_d(k')>_{k'} = 0. \tag{3}$$

On the other hand, if the phonon potential $V_{ph}(k, k')$ represents a forward-scattering phonon, namely, a dominantly stronger potential when the angle (θ) between $\vec{k}$ and $\vec{k'}$ is smaller than a certain angle, say, $|\theta| < \pi/4$, it is obvious that

$$< V_{ph}(k, k')\Delta_d(k') >_{k'} \neq 0, \tag{4}$$

so that the attractive phonon interaction cooperates with the repulsive spin fluctuation interaction $V_{sf}(k, k')$ in Eq. (1) to boost T_c of the d-wave pairing $\Delta_d(k)$[20].

The same mechanism would work for the $s^{\pm}$-wave pairing state. Here the relevant quantity is

$$\sum_{k'} V_{ph}(k, k')[\Delta^+(k') + \Delta^-(k')], \tag{5}$$

where $\Delta^+(k)$ and $\Delta^-(k)$ are the gap functions of the hole and electron bands, respectively, and have opposite signs each other. Let us first consider the special case of an equal size of OPs $|\Delta^+(k')| = |\Delta^-(k')|$. Then the contribution of the local Einstein phonon interaction $V_{ph}(k, k') = V_0$ to the $s^{\pm}$-wave pairing is proportional to

$$V_0 < [\Delta^+(k') + \Delta^-(k')] >_{k'} = 0, \tag{6}$$

hence the phonon boost effect of the ordinary Einstein phonon is null for this non-generic case of the $s^{\pm}$-wave state with the equal size of OPs $|\Delta^+(k')| = |\Delta^-(k')|$. On the other hand, with a forward-scattering phonon, namely, a dominantly stronger potential when $\Delta k = |\vec{k} - \vec{k'}|$ is smaller than the typical distance between the hole band and electron band in the Brillouin zone (BZ), say, $\Delta k < Q = |(\pi, \pi)|$, it is obvious that

$$< V_{ph}(k, k')[\Delta^+(k'_h) + \Delta^-(k'_e)] >_{k'} \neq 0, \tag{7}$$

for any fixed momentum "k" either on the hole FS or on the electron FS. As a result, the forward-scattering phonon interaction boosts the T_c of the $s^{\pm}$-wave state with an equal size of OPs $|\Delta^+(k')| = |\Delta^-(k')|$[21] just as in the case of the d-wave state.

Having illustrated the special case of an equal size of OPs in the $s^{\pm}$-wave state, it is easy to estimate the phonon boost effect on the general $s^{\pm}$-wave pairing state with unequal sizes of OPs $|\Delta^+(k')| \neq |\Delta^-(k')|$. Obviously, the result of Eq. (6) with a local phonon would not be zero if $|\Delta^+(k')| \neq |\Delta^-(k')|$. Hence, we can predict that even a local Einstein phonon can boost the T_c of the general $s^{\pm}$-wave pairing state. In the case of a forward-scattering phonon, we can see that the result of Eq. (7) would be further deviated from zero, hence the phonon boost effect is even more enhanced. The most general expression of calculating the phonon boost effect for the $s^{\pm}$-wave pairing state can be written as,

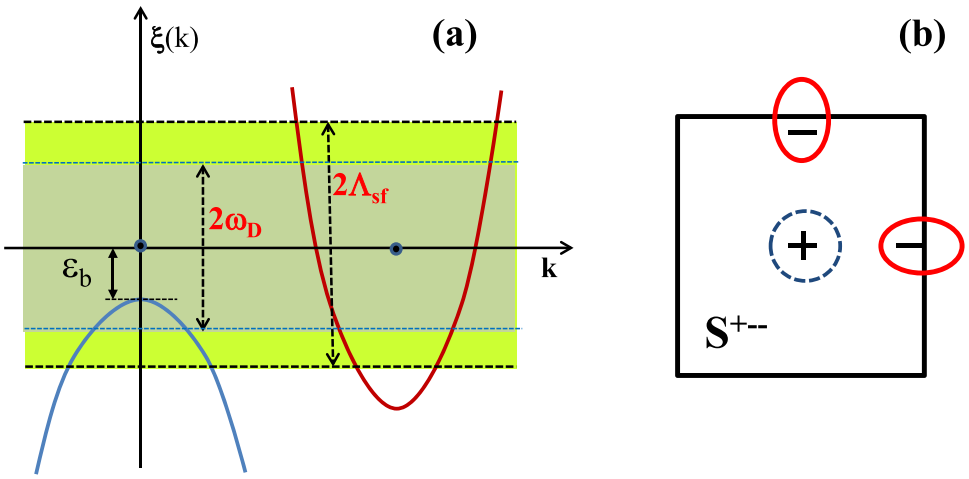

Figure 1. (**a**) A typical incipient band model with $\omega_D < \Lambda_{sf}$. Λ_{sf} is the spin fluctuation energy cutoff and ω_D is the phonon energy cutoff. ω_D can be larger or smaller than ε_b. (**b**) Schematic picture of the Fermi surfaces and the incipient s_{he}^{+-}-wave solution. The hole band has no FS and the dotted circle at Γ point only indicates the SC gap character.

$$< V_{ph}(k, k')[\Delta^{+}(k'_h)\chi^{h}_{ph}(T) + \Delta^{-}(k'_e)\chi^{e}_{ph}(T)] >_{k'} \neq 0. \tag{8}$$

As mentioned already, the sizes of the gap $|\Delta^+|$ and $|\Delta^-|$ are not equal in general when $N_h(0) \neq N_e(0)$[22]. In addition to that, in the case of the incipient band model[14,15,23], the pair susceptibilities $\chi^{h(e)}_{ph}$ can be very different because the integration range of each band is different such as $\chi^{h}_{ph} \sim \int_{-\omega_D}^{-\varepsilon_b} d\xi \cdots$ and $\chi^{e}_{ph} \sim \int_{-\omega_D}^{\omega_D} d\xi \cdots$, respectively, where ε_b is the incipient band distance (see Fig. 1). This effect would enhance the disparity between the hole band and electron band contributions in Eq. (8) even in the case when $N_h(0) = N_e(0)$. Therefore, in the incipient band superconductor, Eq. (8) can be largely deviated from zero and the total contribution to the pairing instability should be

$$\sum_k [< V_{ph}(k, k')[\Delta^{+}(k'_h)\chi^{h}_{ph}(T) + \Delta^{-}(k'_e)\chi^{e}_{ph}(T)] >_{k'}] < 0, \tag{9}$$

assuming an attractive phonon interaction, $V_{ph}(k, k') < 0$. As a result, we expect that any realistic phonons would contribute to increasing the T_c of the $s^{\pm}$-wave state in the incipient band model, regardless of whether the phonon potential $V_{ph}(k, k')$ is from a forward-scattering phonon or a local (all-momentum-scattering) phonon. However, Eq. (9) also tells us that a backward-scattering phonon, that is stronger for larger-momentum exchange, would suppress T_c instead, but we will not consider such an unrealistic phonon. In the following, we studied this phonon-boost effect quantitatively with numerical calculations of T_c of a minimal incipient band model, and confirmed that our speculation is indeed true.

Incipient Band Model. The minimal incipient band model is depicted in Fig. 1. The hole band is sunken below the Fermi level by ε_b, hence it has no FS, and the two electron bands located at X and Y points are treated as one electron band in the minimal two band model. For the pairing interactions, we assumed that the spin fluctuation mediated repulsive interaction $V_{sf}(k, k')(>0)$ is operating within the cutoff energy scale Λ_{sf} and the phonon mediated attractive interaction $V_{ph}(k, k')(<0)$ is operating within the cutoff energy scale ω_D ($<\Lambda_{sf}$). This model has the incipient $s^{\pm}$-wave solution as the most stable SC ground state[14,15] as depicted in Fig. 1(b).

For simplicity of calculations but without loss of generality, we simplify the momentum dependent pairing interactions $V_{sf(ph)}(k, k')$ as the 2×2 matrix potentials depicting the intra-band and inter-band interactions $V^{ab}_{sf(ph)}$, $(a, b = h, e)$, then the T_c-equation of the incipient two band model is written as

$$\begin{aligned} \Delta_h &= [V^{hh}_{sf}\chi^{h}_{sf} + V^{hh}_{ph}\chi^{h}_{ph}]\Delta_h + [V^{he}_{sf}\chi^{e}_{sf} + V^{he}_{ph}\chi^{e}_{ph}]\Delta_e, \\ \Delta_e &= [V^{ee}_{sf}\chi^{e}_{sf} + V^{ee}_{ph}\chi^{e}_{ph}]\Delta_e + [V^{eh}_{sf}\chi^{h}_{sf} + V^{eh}_{ph}\chi^{h}_{ph}]\Delta_h \end{aligned} \tag{10}$$

where the pair susceptibilities are defined as

$$\begin{aligned} \chi^{h}_{sf(ph)}(T) &= -\frac{N_h}{2}\int_{-\Lambda_{sf(ph)}}^{-\varepsilon_b}\frac{d\xi}{\xi}\tanh(\frac{\xi}{2T}) \\ \chi^{e}_{sf(ph)}(T) &= -N_e\int_{-\Lambda_{sf(ph)}}^{\Lambda_{sf(ph)}}\frac{d\xi}{\xi}\tanh(\frac{\xi}{2T}) \end{aligned} \tag{11}$$

where $\Lambda_{ph} = \omega_D$. Obviously $\chi^{h}_{ph}(T) = 0$ when $\omega_D < \varepsilon_b$.

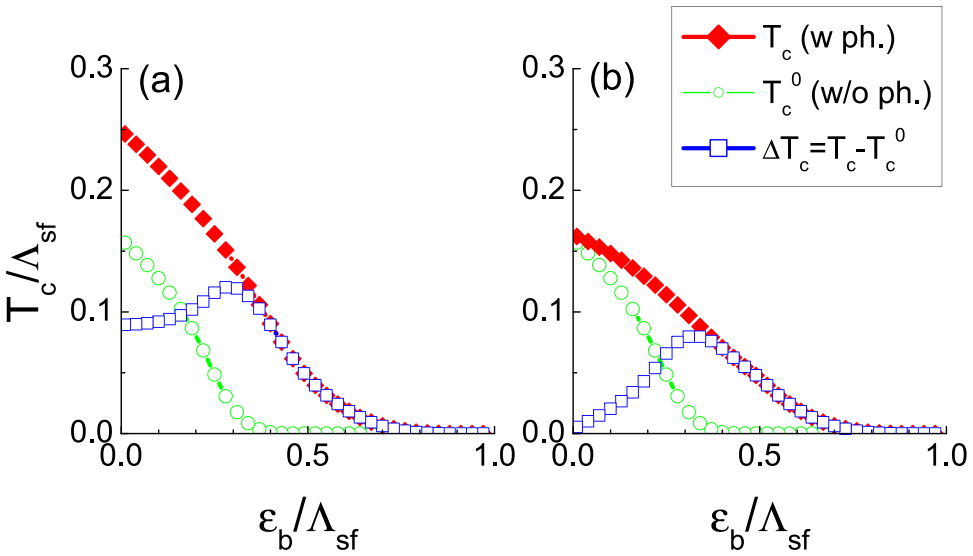

Figure 2. (**a**) Calculated T_c*vs* ε_b of Eq. (9). Green symbols are T_c^0 without the phonon interaction, i.e. $V_{ph}^{ab} = 0$, but only with the spin fluctuation mediated repulsive potential $\sqrt{N_eN_h}\,V_{sf}^{he(eh)} = 1.5$ and $N_{e(h)}V_{sf}^{ee(hh)} = 0.4$. Red diamond symbols are T_c including the additional forward-scattering phonon interaction $N_eV_{ph}^{ee(hh)} = -0.5$ and $\sqrt{N_hN_e}\,V_{ph}^{he(eh)} = 0.0$. The blue square symbols are the net phonon boost effect $\Delta T_c = T_c - T_c^0$. (**b**) The same calculations as (**a**) but with the all-momentum-scattering local phonon interaction $N_eV_{ph}^{ee(hh)} = \sqrt{N_hN_e}\,V_{ph}^{he(eh)} = -0.5$.

Numerical Calculations. First, we calculated the T_c^0 as a function of ε_b without phonon interaction, i.e. $V_{ph}^{ab} = 0$, but only with spin fluctuation mediated repulsive potential $V_{sf}^{ab}(>0)$. We used representative values of the spin-fluctuation mediated repulsive potential $\sqrt{N_eN_h}\,V_{sf}^{he(eh)} = 1.5$ and $N_{e(h)}V_{sf}^{ee(hh)} = 0.4$, and assumed $N_e = N_h$ in all our calculations in this paper. The result of T_c^0 is the green circle symbols in Fig. 2(a,b). T_c^0 gradually decreases as ε_b increases as expected[14,15].

Now we turn on the attractive phonon interaction $V_{ph}^{ab}(<0)$ in addition to the repulsive spin fluctuation interaction V_{sf}^{ab}. We assume the Debye frequency $\omega_D = 0.5\Lambda_{sf}$ for all calculations in this paper. We first test a forward-scattering phonon, i.e. $N_eV_{ph}^{he(eh)} = 0.0$ and $N_eV_{ph}^{ee(hh)} = -0.5$. The results of the calculated T_c are the solid diamond symbols (red) in Fig. 2(a). Apparently, T_c is enhanced almost uniformly from T_c^0. To see more details, we extracted the net amount of the phonon boost effect of T_c as $\Delta T_c = T_c - T_c^0$, which is plotted by the blue square symbols in Fig. 2(a). Interestingly, the phonon boost effect of the purely forward-scattering phonon shows an interesting dependence on ε_b; it peaks roughly when the T_c^0 collapses to zero. This behavior tells us a complicated role of the phonon interaction for the total pairing instability. First, the fact that ΔT_c is always >0 definitely proves that the phonon interaction cooperates with the spin-fluctuation mediated interaction to increase T_c. However, the fact that ΔT_c has a maximum peak near when T_c^0 approaches zero indicates that there is also a subtle competition (or cancellation) between the attractive phonon interaction $V_{ph}^{ee(hh)}(<0)$ and the repulsive spin-fluctuation mediated interaction $V_{sf}^{ee(hh)}(>0)$. However, this competition is confined within the intra-band interactions for the forward-scattering phonon and rather weak. Other than this detail, the results of Fig. 2(a) confirms the well known concept of the forward-scattering phonon boost effect of T_c in the unconventional superconductor with a sign-changing gap function.

Next, we test an Einstein local phonon (all-momentum-scattering phonon), i.e., $\sqrt{N_eN_h}\,V_{ph}^{he(eh)} = N_{e(h)}V_{ph}^{ee(hh)} = -0.5$. The calculated T_c is plotted in Fig. 2(b) as the red diamond symbols. Surprisingly it shows that the local phonon also always enhances T_c from T_c^0 for all values of ε_b. To see more details, the net phonon boost effect $\Delta T_c = T_c - T_c^0$ (blue squares) is plotted. It is about the same magnitude as the pure forward-scattering phonon case except the region where ε_b is small. When ε_b is small, the sizes of the OPs are close each other as $|\Delta_h^+| \sim |\Delta_e^-|$, so that the local phonon contribution in Eq. (8) becomes close to 0, hence the T_c-boost effect of a local phonon is very weak. As ε_b increases, the net phonon boost effect $\Delta T_c = T_c - T_c^0$ increases until it reaches the maximum and eventually decreases. ΔT_c increases because the gap size disparity $|\Delta_h^+|/|\Delta_e^-|$ increases as the hole band sinks deeper. Beyond crossing a certain depth as $\varepsilon_b > \varepsilon_b^*$ (the value ε_b^* where T_c^0 approaches zero), both ΔT_c and T_c itself decreases because the absolute phase space for the pairing interaction shrinks to zero except the intra-electron-band scattering. This is a totally unexpected result contrary to the common belief that *"the forward-scattering is the necessary condition for the phonon boost effect."* Our result of Fig. 2(b) is a clear demonstration that any type of phonon should contribute to enhance T_c, and the sunken band in the incipient band superconductor plays an active role for this unusual behavior.

To see more details, we calculated the T_c with the different values of the phonon interaction strength for each case. The strength of the spin-fluctuation interaction V_{sf}^{ab} is fixed as the same values used in Fig. 2 in all calcula-

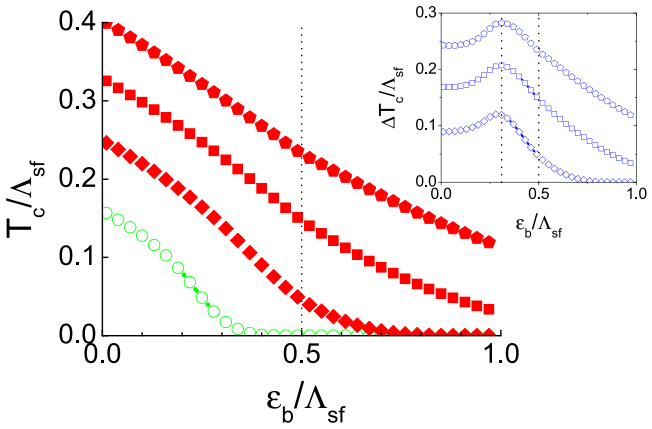

Figure 3. The forward-scattering phonon boost effect. The repulsive spin-fluctuation mediated interaction $\sqrt{N_e N_h}\, V_{sf}^{he(eh)} = 1.5$ and $N_{e(h)} V_{sf}^{ee(hh)} = 0.4$ is fixed for all calculations. The forward-scattering phonon interaction is varied as $N_e V_{ph}^{ee(hh)} = 0.0, -0.5, -1.0$, and -1.5, respectively, in increasing order of T_c, and the inter-band phonon interaction $\sqrt{N_h N_e}\, V_{ph}^{he(eh)} = 0.0$ for all cases. The inset is the plot of the net phonon boost effect $\Delta T_c = T_c - T_c^0$. Vertical lines of $\varepsilon_b^* = 0.32\Lambda_{sf}$ and $\varepsilon_b = \omega_D = 0.5\Lambda_{sf}$ are guides for eyes.

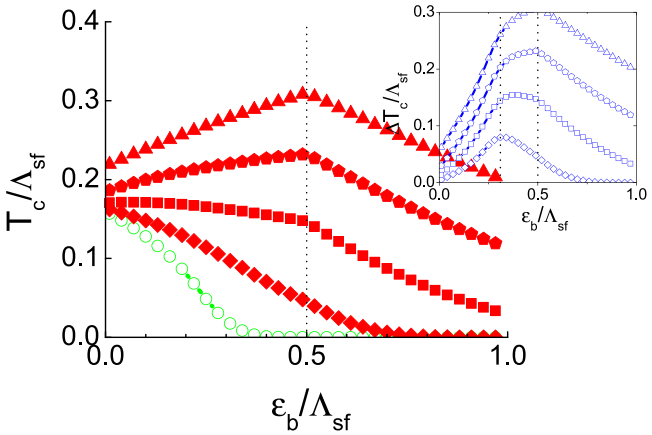

Figure 4. The all-momentum-scattering phonon boost effect. The repulsive spin-fluctuation mediated interaction $\sqrt{N_e N_h}\, V_{sf}^{he(eh)} = 1.5$ and $N_{e(h)} V_{sf}^{ee(hh)} = 0.4$ is fixed for all calculations. The all-momentum-scattering phonon interaction, $N_e V_{ph}^{ee(hh)} = \sqrt{N_h N_e}\, V_{ph}^{he(eh)} = \lambda_{ph}$, is varied as $\lambda_{ph} = 0.0, -0.5, -1.0, -1.5$, and -2.0, respectively, in increasing order of T_c. The inset is the plot of the net phonon boost effect $\Delta T_c = T_c - T_c^0$. Vertical lines of $\varepsilon_b^* = 0.32\Lambda_{sf}$ and $\varepsilon_b = \omega_D = 0.5\Lambda_{sf}$ are guides for eyes.

tions. Figure 3 is the results of T_c with the forward-scattering phonon. The main panel is the calculated T_c with different values of the forward-scattering phonon interaction as $N_e V_{ph}^{ee(hh)} = 0.0, -0.5, -1.0$, and -1.5, respectively, in increasing order of T_c, and $\sqrt{N_h N_e}\, V_{ph}^{he(eh)} = 0.0$ for all cases. The inset of Fig. 3 is the net phonon-boost effect $\Delta T_c = T_c - T_c^0$ for each case. The overall behavior is similar in all cases. The magnitude of ΔT_c monotonically increases with the strength of the phonon interaction, and its peak position is always near ε_b^* (see the inset of Fig. 3). On the other hand, there is no noticeable sign in ΔT_c when ε_b crosses the phonon interaction cutoff $\omega_D = 0.5\Lambda_{sf}$; this is not the case with the local (all-momentum-scattering) phonon.

Figure 4 is the results of T_c with the all-momentum-scattering phonon, hence $N_{e(h)} V_{ph}^{ee(hh)} = \sqrt{N_h N_e}\, V_{ph}^{he(eh)} = \lambda_{ph}$ for all calculations. The coupling strength increases as $\lambda_{ph} = 0.0, -0.5, -1.0, -1.5$ and -2.0, respectively, in increasing order of T_c. The increased T_c is the similar magnitude as in the case of the froward-scattering phonon except for the small ε_b region. A new finding is that this small ε_b region is defined as $\varepsilon_b < \varepsilon_b^*$ for weak coupling phonon (see the $\lambda_{ph} = -0.5$ data in the inset of Fig. 4). Increasing the coupling strength, this small ε_b region, where ΔT_c is increasing as ε_b increases, extends to $\varepsilon_b < \omega_D$. This behavior can be clearly seen by comparing the insets of Figs 3 and 4. The ΔT_c of the forward-scattering phonon case in Fig. 3 has always the maximum peak at $\varepsilon_b = \varepsilon_b^* \approx 0.32$. On the other hand, the peak position of ΔT_c of the all-momentum-scattering phonon case in Fig. 4 shifts from $\varepsilon_b = \varepsilon_b^* \approx 0.32$ to $\varepsilon_b = \omega_D = 0.5$ as the phonon coupling increases. As a result, when the phonon coupling strength is strong enough such as $\lambda_{ph} = -1.5$ and -2.0, the increasing slope of ΔT_c is so steep that the total T_c itself develops a maximum peak at $\varepsilon_b = \omega_D$ and decreases afterwards. This behavior of T_c *vs* ε_b is very different from a standard incipient band model without phonon where T_c monotonically decreases as ε_b increases. Lastly, the T_c boost effect ΔT_c becomes

qualitatively the same as in Fig. 3. when $\varepsilon_b > \omega_D$ (i.e. $\varepsilon_b/\Lambda_{sf} > 0.5$). This behavior is natural to understand because the all-momentum-scattering local phonon cannot mediate the inter-band scattering when $\varepsilon_b > \omega_D$ (see Fig. 1(a)), hence it effectively acts as an "forward-scattering" phonon.

One last remark is that while the calculated T_c in this paper is always of the s_{he}^{+-}-wave solution as depicted in Fig. 1(b), we have also checked the possibility of the s_{he}^{++}-wave solution and we found that it never be a solution with all parameter choices of this paper.

Discussion

We have studied the phonon boost effect on the s_{he}^{+-}-pairing state of the incipient two band model. We have considered both the forward-scattering phonon and the all-momentum-scattering local phonon. It is confirmed that the forward-scattering phonon is efficient to boost T_c. Our model calculations also demonstrated that the optimal condition of the forward-scattering phonon for increasing T_c is to limit its *"forwardness"* narrower than the inter-band distance but wide enough to cover the intra-band scattering of the FSs of each of the electron and hole band.

The most important result of our study is that the all-momentum-scattering local phonon can be an effective T_c-booster as much as the forward-scattering phonon. This surprising result is, in fact, a natural consequence of the intrinsic property of the incipient band model, where a normal band (crossing the Fermi level) and an incipient band (sunken below the Fermi level) severely break the balance between the gap sizes of Δ_h^+ and Δ_e^- on each band. This severe gap size disparity turns the all-momentum-scattering local phonon into an effective forward-scattering phonon. Since this gap size disparity is growing as the incipient band sinks deeper, the phonon-boost effect of the local phonon increases as ε_b increases until ε_b reaches to ε_b^* or ω_D depending on the phonon coupling strength.

Finally, our finding sheds a completely new light on the role of phonon interaction in the Fe-based superconductors, in particular, in the heavily electron-doped iron selenide (HEDIS) compounds. The immediate implication to the FeSe/STO monolayer system is that all interface phonons[12] (both 90 meV and 60 meV F-K phonons) from the STO substrate–regardless of being forward-scattering phonon or not–as well as all intrinsic phonons inside the FeSe-layer itself should contribute to increasing T_c of the FeSe/STO monolayer system, if the pairing gap symmetry is the s_{he}^{+-}-wave state. Besides the FeSe/STO monolayer system, other HEDIS compounds such as $A_xFe_{2-y}Se_2$ (A = K, Rb, Cs, Tl, etc.) ($T_c \approx 30$–$40\,K$)[16–18] and $(Li_{1-x}Fe_xOH)FeSe$ ($T_c \approx 40\,K$)[19], which all develop a deeply sunken ($\varepsilon_b \sim 60$–$90\,meV$) incipient band by electron doping, should also have the phonon-boost effect from the intrinsic phonons in the bulk regardless of their "forwardness" or "local" characters. Our theory can be tested by the isotope effect measurement of the major phonon(s) with O isotope on $SrTiO_3$ substrate and Se isotope for FeSe bulk. Lastly, but not least, although the current paper has studied the electron doped system, i.e., HEDIS, the phonon boost mechanism found in this paper should equally apply to the heavily hole doped system, too, because the principle of the all-phonon boost effect on the s_{he}^{+-}-pairing state relies only on the disparity between the hole band and the electron band.

References

1. Wang, Q. *et al.* Interface-induced high-temperature superconductivity in single unit-cell FeSe films on $SrTiO_3$. *Chin. Phys. Lett.* **29**, 037402 (2012).
2. He, S. *et al.* Phase diagram and electronic indication of high-temperature superconductivity at 65 K in single-layer FeSe films. *Nat. Mater.* **12**, 605 (2013).
3. Ge, J.-F. *et al.* Superconductivity above 100 K in single-layer FeSe films on doped $SrTiO_3$. *Nat. Mater.* **14**, 285 (2014).
4. Stewart, G. R. Superconductivity in iron compounds. *Rev. Mod. Phys.* **83**, 1589–1652 (2011).
5. Hirschfeld, P. J., Korshunov, M. M. & Mazin, I. I. Gap symmetry and structure of Fe-based superconductors. *Reports on Prog. Phys.* **74**, 124508 (2011).
6. Chubukov, A. V. & Hirschfeld, P. J. *Phys. Today* **68**, 46 (2015).
7. Lee, J. J. *et al.* Interfacial mode coupling as the origin of the enhancement of *Tc* in FeSe films on $SrTiO_3$. *Nat.* **515**, 245 (2014).
8. Xiang, Y.-Y., Wang, F., Wang, D., Wang, Q.-H. & Lee, D.-H. High-temperature superconductivity at the FeSe/$SrTiO_3$ interface. *Phys. Rev. B* **86**, 134508 (2012).
9. Lee, D.-H. What makes the *Tc* of FeSe/$SrTiO_3$ so high? *Chin. Phys. B* **24**, 117405 (2015).
10. Rademaker, L., Berlijn, T., Steve, J. & Wang, Y. Enhanced superconductivity due to forward scattering in FeSe thin films on $SrTiO_3$ substrates. *New J. Phys.* **18**, 022001 (2016).
11. Wang, Y., Rademaker, L., Berlijn, T., Nakatsukasa, K. & Johnston, S. Aspects of electron–phonon interactions with strong forward scattering in FeSe thin films on $SrTiO_3$ substrates. *Supercond. Sci. Technol.* **29**, 054009 (2016).
12. Zhang, S. *et al.* Role of $SrTiO_3$ phonon penetrating into thin FeSe films in the enhancement of superconductivity. *Phys. Rev. B* **94**, 081116 (2016).
13. Li, F. & Sawatzky, G. A. Electron phonon coupling versus photoelectron energy loss at the origin of replica bands in photoemission of FeSe on $SrTiO_3$. *Phys. Rev. Lett.* **120**, 237001 (2018).
14. Bang, Y. A shadow gap in the over-doped $(Ba_{1-x}K_x)Fe_2As_2$ compound. *New J. Phys.* **16**, 023029 (2014).
15. Chen, X., Maiti, S., Linscheid, A. & Hirschfeld, P. J. Electron pairing in the presence of incipient bands in Iron-based superconductors. *Phys. Rev. B* **92**, 224514 (2015).
16. Guo, J. *et al.* Superconductivity in the Iron selenide $K_xFe_2Se_2$ ($0 \le x \le 1.0$). *Phys. Rev. B* **82**, 180520 (2010).
17. Wang, A. F. *et al.* Superconductivity at 32 K in single-crystalline $Rb_xFe_{2-y}Se_2$. *Phys. Rev. B* **83**, 060512 (2011).
18. Zhang, Y. *et al.* Nodeless superconducting gap in $A_xFe_2Se_2$ (A=K, Cs) revealed by angle-resolved photoemission spectroscopy. *Nat. Mater.* **10**, 273 (2011).
19. Lu, X. F. *et al.* Coexistence of superconductivity and antiferromagnetism in $(Li_{0.8}Fe_{0.2})$OHFeSe. *Nat. Mater.* **14**, 325 (2014).
20. Bang, Y. Effects of phonon interaction on pairing in high-*Tc* superconductors. *Phys. Rev. B* **78**, 075116 (2008).
21. Bang, Y. Isotope effect and the role of phonons in the Iron-based superconductors. *Phys. Rev. B* **79**, 092503 (2009).
22. Bang, Y. & Choi, H.-Y. Possible pairing states of the Fe-based superconductors. *Phys. Rev. B* **78**, 134523 (2008).
23. Bang, Y. Pairing mechanism of heavily electron doped fese systems: dynamical tuning of the pairing cutoff energy. *New J. Phys.* **18**, 113054 (2016).

Acknowledgements
The author acknowledges the useful discussions on this work with Prof. Young Kuk and Prof. Han-Yong Choi. This work was supported by NRF Grant 2016-R1A2B4-008758 funded by the National Research Foundation of Korea.

Additional Information
Competing Interests: The author declares no competing interests.

Publisher's note: Springer Nature remains neutral with regard to jurisdictional claims in published maps and institutional affiliations.